

# Synthesis and Characterization of Four New Europium Group XIV Chalcogenides: $K_2EuTSe_5$ and $KEuTS_4$ (T = Si, Ge)

Carl R. Evenson, IV and Peter K. Dorhout\*

Department of Chemistry, Colorado State University, Fort Collins, Colorado 80523

Received November 14, 2000

Four europium group XIV chalcogenides have been synthesized using the reactive flux method:  $K_2EuTSe_5$  (**I**, **II**) and  $KEuTS_4$  (**III**, **IV**) where T = Si, Ge.  $K_2EuSiSe_5$ , **I**, crystallizes in the monoclinic space group  $P2_1/c$  with cell parameters  $a = 11.669(3)$  Å,  $b = 9.844(2)$  Å,  $c = 8.917(2)$  Å,  $\beta = 91.583(5)^\circ$ , and  $Z = 4$ .  $K_2EuGeSe_5$ , **II**, crystallizes in the monoclinic space group  $P2_1/c$  with cell parameters  $a = 11.8056(3)$  Å,  $b = 9.9630(1)$  Å,  $c = 8.9456(1)$  Å,  $\beta = 91.195(1)^\circ$ , and  $Z = 4$ . Both  $K_2EuSiSe_5$  and  $K_2EuGeSe_5$  are semiconductors with optical band-gaps of approximately 2.00 and 1.84 eV, respectively. Raman spectroscopy shows vibrations from the  $(TSe_5)^{4-}$  (T = Si, Ge) unit.  $KEuSiS_4$ , **III**, crystallizes in the monoclinic space group  $P2_1$  with cell parameters  $a = 6.426(4)$  Å,  $b = 6.582(5)$  Å,  $c = 8.566(7)$  Å,  $\beta = 107.83(6)^\circ$ , and  $Z = 2$ .  $KEuGeS_4$ , **IV**, crystallizes in the monoclinic space group  $P2_1$  with cell parameters  $a = 6.510(2)$  Å,  $b = 6.649(2)$  Å,  $c = 8.603(3)$  Å,  $\beta = 107.80(2)^\circ$ , and  $Z = 2$ . Band-gap analysis shows that both compounds are semiconductors with optical band-gaps of 1.72 and 1.71 eV, respectively. The Raman spectrum of  $KEuGeS_4$  shows the vibrations of the  $(GeS_4)^{4-}$  unit. Fluorescence spectroscopy confirms the presence of Eu(III) in **III** and **IV** instead of Eu(II) as in **I** and **II**. These four crystalline products were formed under equivalent stoichiometric reaction conditions. The fact that two different products are observed can be used to understand the relationship between the oxidative and reductive potentials within these flux reactions.

## Introduction

In previous papers, we described the use of ternary reaction phase diagrams as an aid in the rational synthesis of quaternary rare-earth chalcophosphate compounds.<sup>1,2</sup> In those papers, different quaternary compounds were found by varying the stoichiometries of reactants. This allowed us to describe the reaction conditions necessary to synthesize products with specific polychalcophosphate units such as  $(PQ_4)^{3-}$  and  $(P_2Q_6)^{4-}$  (Q = S, Se). In addition to looking at the effects of different rare-earth elements on reaction products in these flux reactions we also can vary the main group metal used. Reactive flux chemistry has been described extensively elsewhere.<sup>3–5</sup>

There have been a wide variety of ternary alkali-metal group XIV chalcogenide compounds reported including  $K_4Sn_3Se_8$ ,<sup>6</sup>  $Cs_2Sn_3Se_7$ ,<sup>7</sup>  $K_2Sn_2Se_5$ ,<sup>8</sup>  $K_6Ge_2Q_6$  (Q = S, Se),<sup>9</sup>  $K_6Sn_2Se_7$ ,<sup>10</sup>  $Na_6M_2Se_7$  (M = Si, Ge),<sup>11</sup>  $Na_6Si_2Se_8$ ,<sup>12</sup>  $Na_4M_4Se_{10}$  (M = Si, Ge),<sup>13</sup>  $Na_6M_2Se_6$  (M = Si, Ge),<sup>14</sup>  $Na_4GeSe_4$ ,<sup>15</sup>  $K_4Ge_4Se_{10}$ ,<sup>16</sup> and

$K_4SnSe_4$ .<sup>17</sup> Many of these compounds contain the stable building blocks  $(MSe_4)^{4-}$  and  $(M_2Se_6)^{6-}$  (M = Si, Ge, Sn) which are analogous to the  $(PSe_4)^{3-}$  and  $(P_2Se_6)^{4-}$  units found in selenophosphate compounds.<sup>1,18,19</sup> Group XIV metals also form ternary compounds with rare-earth metal (RE) chalcogenides. Several rare-earth tin sulfides including  $Eu_2SnS_5$ ,<sup>20</sup>  $La_2SnS_5$ ,<sup>21</sup>  $Eu_5Sn_3S_{12}$ ,<sup>22</sup>  $Eu_3Sn_2S_7$ , and  $Eu_2SnS_4$ <sup>23</sup> have been reported.

Quaternary compounds containing group XIV elements include  $K_2MnSnSe_4$ ,<sup>24</sup>  $La_6MgGe_2S_{14}$ ,<sup>25</sup>  $Dy_3CuGeSe_7$ ,<sup>26</sup>  $KLnMQ_4$  (Ln = La, Nd, Gd, Y; M = Si, Ge; Q = S, Se),<sup>27</sup>  $KInGeS_4$  and  $KGaGeS_4$ ,<sup>28</sup>  $Na_{0.5}Pb_{1.75}GeS_4$  and  $Li_{0.5}Pb_{1.75}GeS_4$ ,<sup>29</sup>  $Na_8Pb_2-$

\* To whom correspondence should be addressed. E-mail: pkd@LAMAR.colostate.edu. Peter K. Dorhout is a Camille Dreyfus Teacher Scholar and an A. P. Sloan Fellow.

- (1) Evenson, C. R.; Dorhout, P. K. *Inorg. Chem.*, in press.
- (2) Evenson, C. R.; Dorhout, P. K. *Inorg. Chem.*, in press.
- (3) Sunshine, S. A.; Kang, D.; Ibers, J. A. *J. Am. Chem. Soc.* **1987**, *109*, 6202–6204.
- (4) Cody, J. A.; Mansueto, M. F.; Chien, S.; Ibers, J. A. *Mater. Sci. Forum* **1994**, *152–153*, 35–42.
- (5) Kanatzidis, M. G.; Sutorik, A. C. *Prog. Inorg. Chem.* **1995**, *43*, 151–265.
- (6) Sheldrick, W. S. *Z. Naturforsch.* **1988**, *43b*, 249–252.
- (7) Sheldrick, W. S.; Braunbeck, H.-G. *Z. Naturforsch.* **1990**, *45b*, 1643–1646.
- (8) Klepp, K. O. *Z. Naturforsch.* **1992**, *47b*, 197–200.
- (9) Eisenmann, B.; Kieselbach, E.; Schafer, H.; Schrod, H. *Z. Anorg. Allg. Chem.* **1984**, *516*, 49–54.
- (10) Eisenmann, B.; Hansa, J. *Z. Kristallogr.* **1993**, *203*, 303–304.
- (11) Eisenmann, B.; Hansa, J.; Schafer, H. *Rev. Chim. Miner.* **1986**, *23*, 8.

- (12) Eisenmann, B.; Hansa, J.; Schafer, H. *Z. Anorg. Allg. Chem.* **1985**, *526*, 55.
- (13) Eisenmann, B.; Hansa, J.; Schafer, H. *Z. Naturforsch.* **1985**, *40b*, 450.
- (14) Eisenmann, B.; Hansa, J.; Schafer, H. *Mater. Res. Bull.* **1985**, *20*, 1339.
- (15) Klepp, K. O. *Z. Naturforsch.* **1985**, *40b*, 878.
- (16) Eisenmann, B.; Hansa, J. *Z. Kristallogr.* **1993**, *206*, 101–102.
- (17) Klepp, K. O. *Z. Naturforsch.* **1992**, *47b*, 411–417.
- (18) Chondroudis, K.; Kanatzidis, M. G. *Inorg. Chem.* **1998**, *37*, 3792–3797.
- (19) Chondroudis, K.; Kanatzidis, M. G. *Inorg. Chem. Commun.* **1998**, *1*, 55–57.
- (20) Jaulmes, S.; Julein-Pouzol, P.; Laruelle, P.; Guittard, M. *Acta Crystallogr.* **1982**, *B38*, 79–82.
- (21) Guittard, M.; Julien-Pouzol, M.; Jaulmes, S. *Mater. Res. Bull.* **1976**, *11*, 1073–1080.
- (22) Volkonskaya, T. L.; Gorobets, A. G.; Kizhaev, S. A.; Smirnov, I. A.; Tikhonov, V. V.; Guittard, M.; Lavenant, C.; Flahaut, J. *Phys. Status Solidi A* **1980**, *57*, 731–734.
- (23) Flahaut, J.; Laruelle, P.; Guittard, M.; Jaulmes, S.; Julien-Pouzol, M.; Lavenant, C. *J. Solid State Chem.* **1979**, *29*, 125–136.
- (24) Chen, X.; Huang, X.; Fu, A.; Li, J.; Zhang, L.-D.; Guo, H.-Y. *Chem. Mater.* **2000**, *12*, 2385–2391.
- (25) Gitzendanner, R. L.; Spencer, C. M.; DiSalvo, F. J.; Pell, M. A.; Ibers, J. A. *J. Solid State Chem.* **1997**, *131*, 399–404.
- (26) Huang, F. Q.; Ibers, J. A. *Acta Crystallogr.* **1999**, *C55*, 1210–1212.
- (27) Wu, P.; Ibers, J. A. *J. Solid State Chem.* **1993**, *107*, 347–355.
- (28) Wu, P.; Lu, Y. J.; Ibers, J. A. *J. Solid State Chem.* **1992**, *97*, 383–390.

(M<sub>2</sub>S<sub>6</sub>)<sub>2</sub> (M = Si, Ge) and Na<sub>8</sub>Sn<sub>2</sub>(Ge<sub>2</sub>S<sub>6</sub>)<sub>2</sub>,<sup>30</sup> and A<sub>2</sub>Hg<sub>3</sub>M<sub>2</sub>S<sub>8</sub> (A = Cs, Rb; M = Sn, Ge).<sup>31</sup>

Because of the ability of group XIV elements to form compounds with both RE metals and alkali-metals, we have begun to look at silicon and germanium as alternatives for phosphorus in solid-state reactive flux reactions with rare-earth metals. Here we report four new europium group XIV chalcogenides: K<sub>2</sub>EuSiSe<sub>5</sub>, K<sub>2</sub>EuGeSe<sub>5</sub>, KEuSiS<sub>4</sub>, and KEuGeS<sub>4</sub>.

## Experimental Section

**Synthesis.** The following reactants were used as received and stored in an inert atmosphere glovebox: Eu (99.95%, Ames Laboratory), Si (99.999%, Johnson-Mathey), Ge (99.999% Alfa), S (99.999%, Johnson-Mathey), and Se (99.999%, Johnson-Mathey). K<sub>2</sub>S<sub>2</sub> and K<sub>2</sub>Se<sub>4</sub> were previously made in liquid ammonia from the stoichiometric combination of the elements.<sup>32,33</sup> Reactants were loaded into fused silica ampules inside an inert atmosphere glovebox. Each ampule was flame sealed under vacuum and placed in a temperature controlled tube furnace. Compound **I** was ramped to 525 °C where it remained for 150 h. For compounds **II** through **IV** the furnace was ramped to 725 °C where it remained for 150 h. In both cases the furnace was allowed to cool back to room temperature at 4 °C/hr. Compound **I** can be found in reactions at 725 °C but a reaction was done at a lower temperature to obtain better crystals.

K<sub>2</sub>EuSiSe<sub>5</sub>, **I**, was synthesized by combining 44.3 mg (0.561 mmol) of Se, 147.4 mg (0.374 mmol) of K<sub>2</sub>Se<sub>4</sub>, 5.3 mg (0.188 mmol) of Si, and 28.4 mg (0.188 mmol) of Eu. After the reaction product was cooled, it was washed with dimethylformamide (DMF) yielding a binary crystalline product composed of EuSe<sup>34</sup> and orange plates of K<sub>2</sub>EuSiSe<sub>5</sub>.

K<sub>2</sub>EuGeSe<sub>5</sub>, **II**, was synthesized by combining 38.9 mg (0.493 mmol) of Se, 125.4 mg (0.318 mmol) of K<sub>2</sub>Se<sub>4</sub>, 11.9 mg (0.164 mmol) of Ge, and 25.0 mg (0.164 mmol) of Eu. The reaction product was washed with DMF yielding a ternary crystalline product composed of K<sub>2</sub>GeSe<sub>4</sub>,<sup>35</sup> EuSe,<sup>34</sup> and red rods of K<sub>2</sub>EuGeSe<sub>5</sub>.

KEuSiS<sub>4</sub>, **III**, was synthesized by combining 63.2 mg (1.97 mmol) of S, 80.2 mg (0.563 mmol) of K<sub>2</sub>S<sub>2</sub>, 8.1 mg (0.288 mmol) of Si, and 42.8 mg (0.288 mmol) of Eu. Washing the product with DMF yielded brown plates of KEuSiS<sub>4</sub>.

KEuGeS<sub>4</sub>, **IV**, was synthesized by combining 43.1 mg (1.34 mmol) of S, 54.7 mg (0.384 mmol) of K<sub>2</sub>S<sub>2</sub>, 13.9 mg (0.191 mmol) of Ge, and 29.2 mg (0.191 mmol) of Eu. The product was washed with DMF yielding deep red plates of KEuGeS<sub>4</sub>.

**Physical Measurements. Single-Crystal X-ray Diffraction.** Intensity data sets for compounds **I–IV** were collected using a Bruker Smart CCD diffractometer. The intensity data set for **I** was integrated using SAINT-NT,<sup>36</sup> a SADABS correction was applied,<sup>37</sup> and the structure was solved by direct methods using SHELXTL.<sup>38</sup> Intensity data sets for **II–IV** were integrated using SAINT,<sup>39</sup> a SADABS correction was applied,<sup>37</sup> and the structures were solved by direct methods using SHELXTL.<sup>40</sup> Relevant crystallographic data collection and refinement parameters for K<sub>2</sub>EuSiSe<sub>5</sub>, K<sub>2</sub>EuGeSe<sub>5</sub>, KEuSiS<sub>4</sub>, and KEuGeS<sub>4</sub> are reported in Table 1.

**Table 1.** Crystallographic Data for K<sub>2</sub>EuSiSe<sub>5</sub>, K<sub>2</sub>EuGeSe<sub>5</sub>, KEuSiS<sub>4</sub>, and KEuGeS<sub>4</sub>

	K <sub>2</sub> EuSiSe <sub>5</sub> (I)	K <sub>2</sub> EuGeSe <sub>5</sub> (II)	KEuSiS <sub>4</sub> (III)	KEuGeS <sub>4</sub> (IV)
fw	653.05	697.55	347.39	391.89
<i>a</i> , Å	11.669(3)	11.8056(3)	6.426(4)	6.510(2)
<i>b</i> , Å	9.844(2)	9.9630(1)	6.582(5)	6.649(2)
<i>c</i> , Å	8.917(2)	8.9456(1)	8.566(7)	8.603(3)
α, deg	90.0	90.0	90.0	90.0
β, deg	91.583(5)	91.195(1)	107.83(6)	107.80(2)
γ, deg	90.0	90.0	90.0	90.0
<i>V</i> , Å <sup>3</sup>	1023.9(4)	1051.95(3)	344.9(4)	354.5(2)
<i>Z</i>	4	4	2	2
λ(Mo Kα), Å	0.71073	0.71073	0.71073	0.71073
space group	<i>P</i> 2 <sub>1</sub> / <i>c</i> #14	<i>P</i> 2 <sub>1</sub> / <i>c</i> #14	<i>P</i> 2 <sub>1</sub> #4	<i>P</i> 2 <sub>1</sub> #4
temp, K	171(2)	167(2)	170(2)	167(2)
ρ <sub>calc.</sub> , mg/cm <sup>3</sup>	4.236	4.404	3.345	3.671
μ (mm <sup>-1</sup> )	24.751	26.781	10.952	14.645
R1% <sup>a</sup>	5.19	4.36	4.71	3.46
wR2% <sup>a</sup>	11.38	8.31	12.50	8.57

$$^a R1 = \sum(|F_o| - |F_c|) / \sum |F_o|. \quad wR2 = [\sum(w(F_o^2 - F_c^2)^2) / \sum(w(F_o^2)^2)]^{1/2}.$$

**Raman Spectroscopy.** The bulk-single-crystal solid-state Raman spectrum of compounds **I**, **II**, and **IV** were taken with a Nicolet Magna-IR 760 Spectrometer with a FT-Raman Module attachment using a Nd:YAG excitation laser (1064 nm). A Raman spectrum could not be obtained for compound **III** due to sample heating.

**UV–Vis Spectroscopy.** Diffuse reflectance measurements for all compounds were taken with a Varian Cary 500 Scan UV–Vis–NIR spectrophotometer equipped with a Praying Mantis accessory. A polyTeflon standard was used as a reference. The Kubelka–Munk function was applied to obtain band-gap information.<sup>41,42</sup>

**Fluorescence Spectroscopy.** The solid-state low-temperature fluorescence emission spectra of compounds **III** and **IV** were taken on a SPEX Fluorlog-3 spectrofluorometer using bulk powders cooled to liquid nitrogen temperatures.

## Results and Discussion

Compounds **I** and **II** and **III** and **IV** are isostructural; therefore, only the structures of the germanium analogues will be discussed in detail. Important bond distances and angles and thermal ellipsoid figures for **I** and **III** are provided in the Supporting Information.

**K<sub>2</sub>EuTSe<sub>5</sub> I and II.** A single crystal of K<sub>2</sub>EuSiSe<sub>5</sub>, **I**, was selected, 6822 (2477 independent) reflections were collected, and an absorption correction was applied (*R*<sub>int</sub> = 0.0880). The structure was solved in *P*2<sub>1</sub>/*c* by direct methods with final electron density residuals of 2.542 and -2.773 eÅ<sup>-3</sup>, and all atoms were refined anisotropically with SHELXTL using full-matrix least-squares refinement on *F*<sup>2</sup> for 83 variables.<sup>38</sup> Table 2 lists fractional atomic coordinates and isotropic displacement parameters for K<sub>2</sub>EuSiSe<sub>5</sub>.

A single crystal of K<sub>2</sub>EuGeSe<sub>5</sub>, **II**, was selected, 6796 (2518 independent) reflections were collected, and an absorption correction was applied (*R*<sub>int</sub> = 0.0841). The structure was solved in *P*2<sub>1</sub>/*c* by direct methods with final electron density residuals of 2.169 and -2.436 eÅ<sup>-3</sup>, and all atoms were refined anisotropically with SHELXTL using full-matrix least-squares refinement on *F*<sup>2</sup> for 83 variables.<sup>40</sup> Table 2 lists fractional atomic coordinates and isotropic displacement parameters for K<sub>2</sub>EuGeSe<sub>5</sub>.

K<sub>2</sub>EuGeSe<sub>5</sub> is a 2-dimensional layered structure in which 9-coordinate Eu(II) atoms are linked into a layer by (GeSe<sub>5</sub>)<sup>4-</sup> units. This unit, shown in Figure 1, comprises a Ge(IV) tetrahedron with one of its (Se)<sup>2-</sup> corners replaced by a (Se<sub>2</sub>)<sup>2-</sup> unit. This diselenide arm distorts the tetrahedron slightly. Table 3 reports selected bond distances and

(29) Aitken, J. A.; Marking, G. A.; Evain, M.; Iordanidis, L.; Kanatzidis, M. G. *J. Solid State Chem.* **2000**, *153*, 158–169.

(30) Marking, G. A.; Kanatzidis, M. G. *J. Alloys Compd.* **1997**, *259*, 122–128.

(31) Marking, G. A.; Hanko, J. A.; Kanatzidis, M. G. *Chem. Mater.* **1998**, *10*, 1191–1199.

(32) Liao, J.-H.; Kanatzidis, M. G. *Inorg. Chem.* **1992**, *31*, 431–439.

(33) Schewe-Miller, I. *Metallreiche hauptgruppenmetall-Chalkogenverbindungen: Synthese, Strukturen und Eigenschaften*. Ph.D. Thesis, Max-Planck-Institut für Festkörperforschung, Stuttgart, Germany, 1990.

(34) Guittard, M.; Benacerraf, A. *Compt. Rend.* **1959**, *248*, 2589.

(35) Sheldrick, W. S.; Schaaf, B. Z. *Naturforsch. B: Chem. Sci.* **1995**, *50*, 1469–1475.

(36) SAINT-NT V5/6.0; Bruker AXS Inc.: Madison, WI, 1996.

(37) Sheldrick, G. M. *SADABS*; University of Gottingen: Germany, 1997.

(38) SHELXTL 5.1; Bruker AXS Inc.: Madison, WI, 1998.

(39) SAINT; Data processing software for the SMART system; Bruker Analytical X-ray Instruments Inc.: Madison, WI, 1995.

(40) SHELXTL 5.03; Bruker Analytical X-ray Systems Inc.: Madison, WI, 1994.

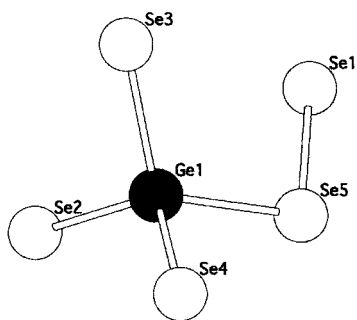
(41) McCarthy, T. J.; Tanzer, T. A.; Kanatzidis, M. G. *J. Am. Chem. Soc.* **1995**, *117*, 1294–1301.

(42) Wilkinson, F.; Kelly, G. In *CRC Handbook of Organic Photochemistry*; Scavano, J. C., Ed.; CRC Press: Boca Raton, FL, 1989; Vol. 1, pp 293–314.

**Table 2.** Fractional Atomic Coordinates and Equivalent Isotropic Displacement Parameters ( $\text{\AA}^2 \times 10^3$ )<sup>a</sup> for  $\text{K}_2\text{EuSiSe}_5$  and  $\text{K}_2\text{EuGeSe}_5$ 

	x	y	z	U(eq)
$\text{K}_2\text{EuSiSe}_5$				
Eu(1)	0.4838(1)	0.7337(1)	0.1029(1)	9(1)
Se(1)	0.4063(1)	0.4363(1)	0.1556(1)	10(1)
Se(2)	0.3977(1)	0.0405(1)	0.1390(1)	9(1)
Se(3)	0.2855(1)	0.7404(1)	-0.1505(1)	11(1)
Se(4)	0.0742(1)	0.0159(1)	0.1947(1)	13(1)
Se(5)	0.7573(1)	0.6220(1)	0.0056(1)	11(1)
Si(1)	0.2526(3)	0.9782(3)	0.2879(3)	8(1)
K(1)	0.8041(2)	0.9419(3)	0.1282(3)	14(1)
K(2)	0.0602(3)	0.6973(3)	0.0443(3)	25(1)
$\text{K}_2\text{EuGeSe}_5$				
Eu(1)	0.4837(1)	0.7306(1)	0.1053(1)	9(1)
Se(1)	0.4079(1)	0.4340(1)	0.1589(1)	10(1)
Se(2)	0.4037(1)	0.0381(1)	0.1352(1)	9(1)
Se(3)	0.2878(1)	0.7446(1)	-0.1428(1)	11(1)
Se(4)	0.0697(1)	0.0143(1)	0.1945(1)	13(1)
Se(5)	0.7532(1)	0.6306(1)	-0.0004(1)	13(1)
Ge(1)	0.2530(1)	0.9793(1)	0.2908(1)	9(1)
K(1)	0.8022(2)	0.9441(2)	0.1257(3)	14(1)
K(2)	0.0559(2)	0.6995(3)	0.0395(3)	27(1)

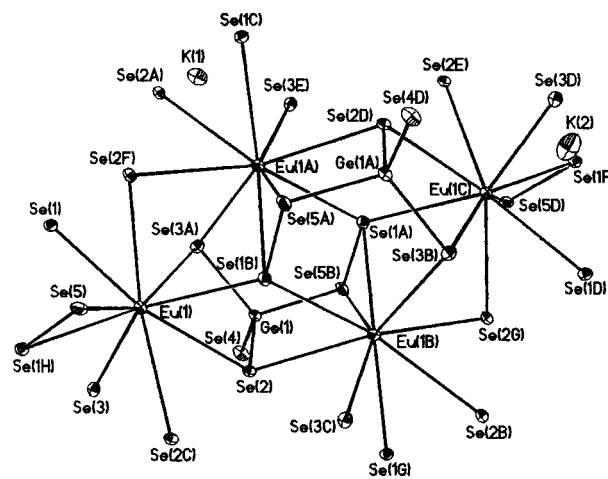
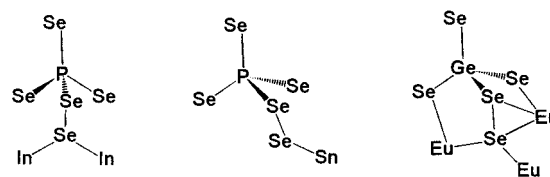
<sup>a</sup> U(eq) is defined as one-third of the trace of the orthogonalized  $U_{ij}$  tensor.

**Figure 1.**  $(\text{GeSe}_5)^{4-}$  unit.**Table 3.** Selected Bond Distances ( $\text{\AA}$ ) and Angles (Deg) for  $\text{K}_2\text{EuGeSe}_5$ 

Eu(1)–Se(1)	3.127(1)	Eu(1)–Se(1')	3.168(1)
Eu(1)–Se(3)	3.174(1)	Eu(1)–Se(1'')	3.174(1)
Eu(1)–Se(2)	3.219(1)	Eu(1)–Se(2')	3.271(1)
Eu(1)–Se(3')	3.272(1)	Eu(1)–Se(2'')	3.438(1)
Eu(1)–Se(5)	3.483(1)	Ge(1)–Se(4)	2.339(2)
Ge(1)–Se(3)	2.342(1)	Ge(1)–Se(2)	2.356(2)
Ge(1)–Se(5)	2.408(1)	Se(5)–Se(1)	2.435(2)
Se(4)–Ge(1)–Se(3)	113.06(6)	Se(4)–Ge(1)–Se(2)	116.72(6)
Se(3)–Ge(1)–Se(2)	104.83(5)	Se(4)–Ge(1)–Se(5)	98.66(5)
Se(3)–Ge(1)–Se(5)	114.00(5)	Se(2)–Ge(1)–Se(5)	109.87(6)
Ge(1)–Se(5)–Se(1)	104.59(5)		

angles in  $\text{K}_2\text{EuGeSe}_5$ . The longest Ge–Se bond length is 2.408(1)  $\text{\AA}$ , and the average Ge–Se bond length is 2.362(3)  $\text{\AA}$ . The Se(5)–Se(1) bond length is 2.435(2)  $\text{\AA}$ , and the Ge(1)–Se(5)–Se(1) bond angle is 104.59(5)°. A structure with a related building block is  $\text{Cs}_4\text{GeTe}_6$ .<sup>43</sup> It contains  $(\text{GeTe}_6)^{4-}$  units with two di-selenide arms. Five different  $(\text{GeSe}_5)^{4-}$  units are coordinated to each europium atom. Two units are bound to europium with one selenium atom, two units are bound with two selenium atoms, and the fifth  $(\text{GeSe}_5)^{4-}$  unit is bound to europium with three of its selenium atoms. Each  $(\text{GeSe}_5)^{4-}$  unit links four different Eu(II) atoms together within a layer as seen in Figure 2.

The  $(\text{TeSe}_5)^{4-}$  anionic unit has been observed before as  $(\text{PSe}_5)^{3-}$ , but to our knowledge the  $(\text{GeSe}_5)^{4-}$  and  $(\text{SiSe}_5)^{4-}$  units have not been found in a rare-earth metal structure. Kanatzidis et al. has reported several

**Figure 2.** ORTEP plot showing the coordination sphere of europium and intricate bonding from  $(\text{GeSe}_5)^{4-}$  units in  $\text{K}_2\text{EuGeSe}_5$ . Thermal ellipsoids are plotted at the 50% probability level.**Scheme 1**

structures with  $(\text{PSe}_5)^{3-}$  anionic units including  $\text{K}_4\text{In}_2(\text{PSe}_5)_2(\text{P}_2\text{Se}_6)$  and  $\text{Rb}_3\text{Sn}(\text{PSe}_5)(\text{P}_2\text{Se}_6)$ <sup>44</sup> and  $\text{Rb}_3\text{Sn}(\text{PSe}_5)_3$ .<sup>45</sup> The  $(\text{PSe}_5)^{3-}$  unit in these structures is similar to the  $(\text{GeSe}_5)^{4-}$  unit, however, the interactions of  $(\text{PSe}_5)^{3-}$  with tin or indium is very different from that found in  $\text{K}_2\text{EuGeSe}_5$ . In both  $\text{K}_4\text{In}_2(\text{PSe}_5)_2(\text{P}_2\text{Se}_6)$  and  $\text{Rb}_3\text{Sn}(\text{PSe}_5)(\text{P}_2\text{Se}_6)$  the  $(\text{PSe}_5)^{3-}$  units only bond to indium or tin, respectively, with the second selenium atom in the di-selenide arm (see Scheme 1). In contrast, both selenium atoms on the di-selenide arm in  $(\text{GeSe}_5)^{4-}$  are intricately bound to europium atoms in  $\text{K}_2\text{EuGeSe}_5$ .

The  $[\text{Eu}(\text{GeSe}_5)_2]^{2-}$  layers in  $\text{K}_2\text{EuGeSe}_5$  lie parallel to the (011) plane. Layers are separated from one another by potassium cations resulting in a van der Waals gap of 3.828  $\text{\AA}$ . The bonding in these layers is quite intricate with selenium atoms bonding to several europium atoms within the layer. The 9-coordinate europium atoms have an average Eu–Se bond length of 3.323(3)  $\text{\AA}$ . The shortest Eu–Se bond is from Se(1), which bonds to three different europium atoms as seen in Figure 2. Se(4) is the only terminal selenium that points into the gap between layers. The europium site occupancy was allowed to freely vary to test for the possibility of Eu(III) in this structure; that is, partially occupied Eu(III) sites could charge balance the structure as would a fully occupied Eu(II) site. It was found that the occupancy was exactly 1, indicating a structure with only Eu(II).

**KEuTS<sub>4</sub> III and IV.** A single crystal of  $\text{KEuSi}_4$ , **III**, was selected, 2293 (1536 independent) reflections were collected, and an absorption correction was applied ( $R_{\text{int}} = 0.0512$ ). The structure was solved in  $P2_1$  by direct methods to electron density residuals of 2.234 and  $-2.739 \text{ e}\text{\AA}^{-3}$ , and all atoms were refined anisotropically with SHELXTL using full-matrix least-squares refinement on  $F^2$  for 64 variables.<sup>40</sup> Table 4 lists fractional atomic coordinates and isotropic displacement parameters for  $\text{KEuSi}_4$ . PLATON<sup>46</sup> suggested  $P2_1/m$  as the correct space group, however, the structure could not be solved in the centrosymmetric space group. Comparison of Friedel pairs confirmed the noncentrosymmetric space group.

(44) Chondroudis, K.; Kanatzidis, M. G. *J. Solid State Chem.* **1998**, *136*, 79–86.

(45) Chondroudis, K.; Kanatzidis, M. G. *Chem. Commun.* **1996**, 1371–1372.

(46) Spek, A. L. *PLATON32*; Department of Chemistry, Utrecht University: The Netherlands, 2000.

(43) Brinkmann, C.; Eisenmann, B.; Schafer, H. *Mater. Res. Bull.* **1985**, *20*, 1207–1211.



**Table 4.** Fractional Atomic Coordinates and Equivalent Isotropic Displacement Parameters ( $\text{\AA}^2 \times 10^3$ )<sup>a</sup> for KEuSiS<sub>4</sub> and KEuGeS<sub>4</sub>

	x	y	z	U(eq)
KEuSiS <sub>4</sub>				
Eu(1)	0.2701(1)	0.0000	0.9493(1)	6(1)
Si(1)	0.7165(6)	0.0332(5)	0.8200(4)	6(1)
S(1)	0.4795(5)	-0.7308(5)	0.7733(5)	8(1)
S(2)	0.4811(5)	-0.7302(5)	0.2095(4)	6(1)
S(3)	-0.0884(5)	-0.9661(5)	0.6645(4)	8(1)
S(4)	0.0858(5)	-0.4207(5)	0.9343(4)	7(1)
K(1)	0.2251(5)	0.0202(7)	0.4340(3)	16(1)
KEuGeS <sub>4</sub>				
Eu(1)	0.2698(1)	0.0000	0.9475(1)	6(1)
Ge(1)	0.7208(1)	0.0344(1)	0.8208(1)	5(1)
S(1)	0.4741(4)	-0.7268(4)	0.7753(3)	7(1)
S(2)	0.4843(3)	-0.7362(4)	0.2084(3)	6(1)
S(3)	-0.0792(3)	-0.9635(4)	0.6589(3)	10(1)
S(4)	0.0729(3)	-0.4075(4)	0.9270(3)	7(1)
K(1)	0.2329(3)	0.0179(5)	0.4361(2)	15(1)

<sup>a</sup> U(eq) is defined as one-third of the trace of the orthogonalized U<sub>ij</sub> tensor.

**Table 5.** Selected Bond Distances ( $\text{\AA}$ ) for KEuGeS<sub>4</sub>

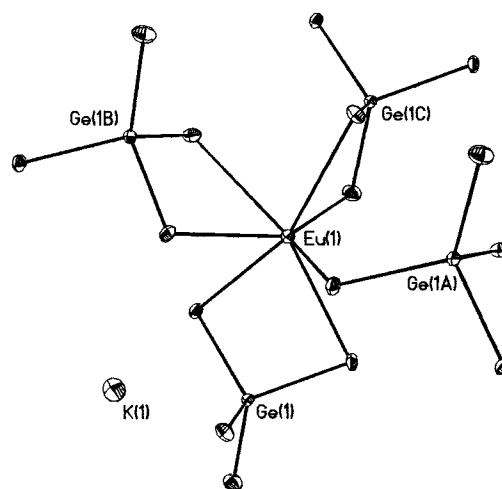
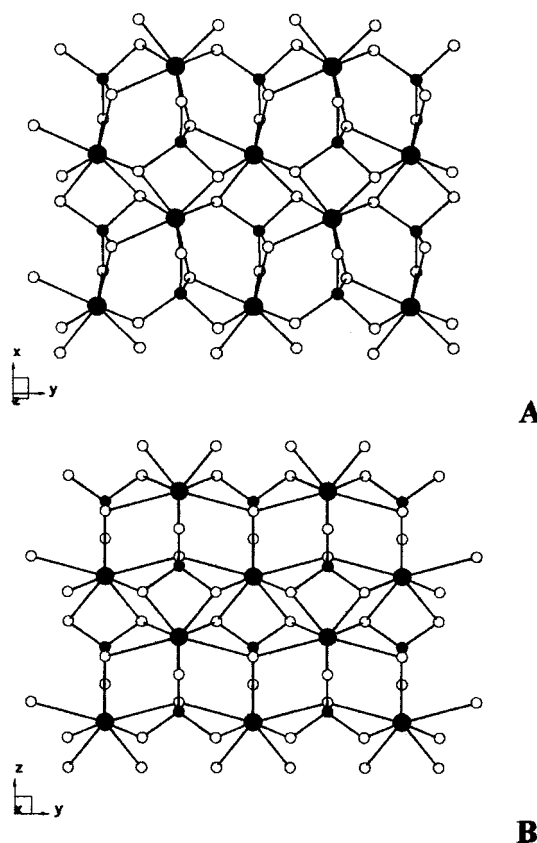
Eu(1)–S(3)	2.817(2)	Ge(1)–S(1)	2.206(2)
Eu(1)–S(2')	2.853(2)	Ge(1)–S(2)	2.208(3)
Eu(1)–S(1')	2.882(2)	Ge(1)–S(3)	2.178(2)
Eu(1)–S(4)	2.979(3)	Ge(1)–S(4)	2.209(2)
Eu(1)–S(4')	2.828(2)		
Eu(1)–S(2)	2.854(2)		
Eu(1)–S(1)	2.910(3)		

A single crystal of KEuGeS<sub>4</sub>, **IV**, was selected, 2400 (1572 independent) reflections were collected, and an absorption correction was applied ( $R_{\text{int}} = 0.0355$ ). The structure was solved in  $P2_1$  by direct methods to electron density residuals of 2.656 and  $-2.591 \text{ e\AA}^{-3}$ , and all atoms were refined anisotropically with SHELXTL using full-matrix least-squares refinement on  $F^2$  for 64 variables.<sup>40</sup> Table 4 lists fractional atomic coordinates and isotropic displacement parameters for KEuGeS<sub>4</sub>. A related compound, KEuPS<sub>4</sub>,<sup>2</sup> crystallized in the  $P2_1/c$  space group so we assumed a centrosymmetric solution. Systematic absence analysis suggested either  $P2_1/m$  or  $P2_1$  as possible space groups, however, the structure could not be solved in the centrosymmetric space group. Selected bond lengths for KEuGeS<sub>4</sub> are reported in Table 5.

KEuGeS<sub>4</sub> is isostructural to KLaGeS<sub>4</sub>.<sup>27</sup> While the structure is not new, it is of interest to us because of the Eu(III) cation and the comparisons we will make to compounds **I** and **II** containing Eu(II). KEuGeS<sub>4</sub> is a two-dimensional structure with  ${}^2[\text{Eu}(\text{GeS}_4)]^-$  layers separated by potassium cations. Within each layer, seven-coordinate distorted monocapped trigonal prisms of Eu(III)S<sub>7</sub> are linked together by distorted  $(\text{GeS}_4)^{4-}$  tetrahedra. Figure 3 shows that each europium atom is coordinated by three  $(\text{GeS}_4)^{4-}$  units in an edge-sharing manner and bonded to a fourth  $(\text{GeS}_4)^{4-}$  tetrahedron in a corner-sharing manner. The average Eu–S bond length is 2.875(6)  $\text{\AA}$ . Each  $(\text{GeS}_4)^{4-}$  tetrahedron bonds to three Eu(III) atoms in an edge-sharing manner and to a fourth Eu(III) in a corner-sharing manner.

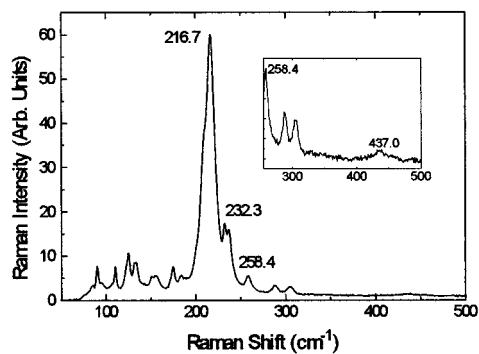
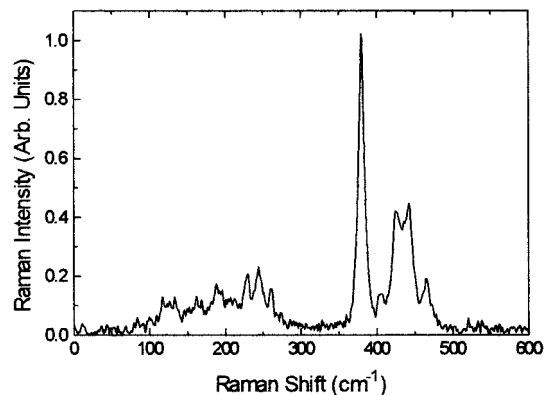
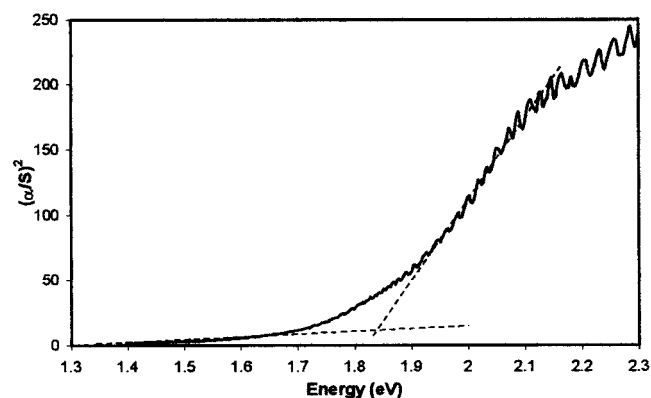
The structure of KEuGeS<sub>4</sub> is very similar to KEuPS<sub>4</sub><sup>2</sup> with some significant differences. Figure 4 shows packing diagrams for KEuGeS<sub>4</sub> and KEuPS<sub>4</sub>. The noncentrosymmetric nature of KEuGeS<sub>4</sub> can clearly be seen compared to the centrosymmetric KEuPS<sub>4</sub> structure. The europium trigonal prisms in KEuGeS<sub>4</sub> are capped on only one side, while the europium trigonal prisms in KEuPS<sub>4</sub> are capped on both sides. The average Eu–S bond length in KEuGeS<sub>4</sub> and KEuPS<sub>4</sub> can be used to show the effect of Eu(III) vs Eu(II) in these two structures. KEuPS<sub>4</sub> has an average Eu(II)–S bond length of 3.127(5)  $\text{\AA}$  while KEuGeS<sub>4</sub> has an average Eu(III)–S bond length of 2.875(6)  $\text{\AA}$ . This shorter average bond length is expected in a compound with Eu(III) instead of Eu(II).

By comparing compounds **I** and **II** to **III** and **IV** we can see the effect of using sulfur as an oxidizing agent in the flux reaction instead of selenium. All four reactions were done under nearly equivalent flux reaction stoichiometries. In K<sub>2</sub>EuSiSe<sub>5</sub> and K<sub>2</sub>EuGeSe<sub>5</sub> europium exists

**Figure 3.** ORTEP plot of the coordination environment around europium in KEuGeS<sub>4</sub>. Thermal ellipsoids plotted at the 50% probability level.**Figure 4.** Packing diagram of (A) KEuGeS<sub>4</sub> and (B) KEuPS<sub>4</sub>. Large filled circles are europium atoms, small filled circles are germanium or phosphorus atoms, and open circles are sulfur atoms. Potassium atoms have been removed.

as Eu(II) and Se–Se bonding is observed. The analogous sulfur reactions yield structures with Eu(III) and no S–S bonding in KEuSiS<sub>4</sub> and KEuGeS<sub>4</sub>. This can be rationalized by citing the better oxidizing ability of sulfur versus selenium. Other Eu(III) and Eu(II) structures such as EuPO<sub>4</sub> and KEuPO<sub>4</sub><sup>47</sup> can also be found in oxide chemistry, however, these compounds are synthesized under very different reaction conditions and cannot be compared to the chalcogenide flux reactions described here. It is interesting to note that when using phosphorus as

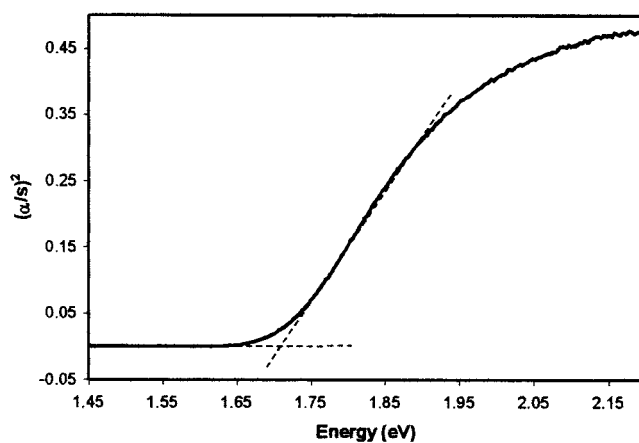
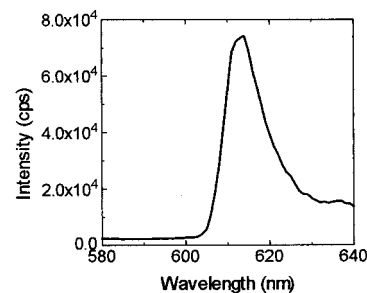
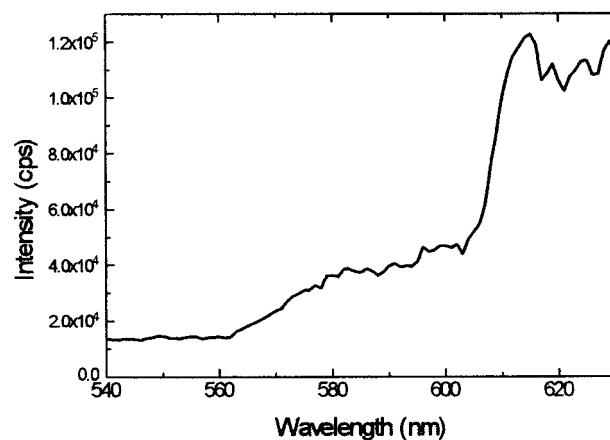
(47) Wu, G.; Tang, Z.; Yu, Y.; Lin, P.; Jansen, M.; Koenigstein, K. Z. *Anorg. Allg. Chem.* **1992**, 610, 135–138.

Figure 5. Raman spectrum of  $K_2EuGeSe_5$ .Figure 6. Raman spectrum of  $KEuGeS_4$ .Figure 7. Optical band-gap of  $K_2EuGeSe_5$ .Table 6. Raman Peaks ( $cm^{-1}$ ) Found in  $K_2EuGeSe_5$  and  $KEuGeS_4$ 

$K_2EuGeSe_5$	$KEuGeS_4$
90.1	117.1
110.3	133.2
125.0	162.0
133.4	188.0
155.7	229.8
174.7	243.9
183.9	259.8
216.7 $\nu_1(A_1)$	379.9 $\nu_1(A_1)$
232.3	425.1
258.4	442.5
287.4	465.1
305.8	
437.0 $\nu_3(F_2)$	

the main group metal, neither the di-selenide unit nor Eu(III) were observed in the reaction products.<sup>1,2</sup>

**Vibrational and Electronic Spectroscopy.** The Raman spectra of  $K_2EuGeSe_5$  and  $KEuGeS_4$  are shown in Figures 5 and 6, respectively. In Figure 5 we observe that the four peaks expected for a normal tetrahedral molecule are not seen due to the distortion of the tetrahedron

Figure 8. Optical band-gap of  $KEuGeS_4$ .Figure 9. Fluorescence emission spectrum for  $KEuSiS_4$ .Figure 10. Fluorescence emission spectrum for  $KEuGeS_4$ .

by the di-selenide arm in  $K_2EuGeSe_5$ . The large peak at  $216.7\text{ cm}^{-1}$  is attributed to the totally symmetric stretch of the distorted  $(GeSe_5)^{4-}$  tetrahedron and the weak peak at  $437.0\text{ cm}^{-1}$  is attributed to the antisymmetric stretch. Se–Se Raman vibrations found in the literature range from  $225\text{ cm}^{-1}$  in  $Rb_3Sn(PSe_5)(P_2Se_6)^{44}$  to  $283\text{ cm}^{-1}$  in  $Cs_4Th_2P_5Se_{17}$ .<sup>48</sup> The peak at  $258.4\text{ cm}^{-1}$  is tentatively assigned to the Se–Se stretching vibration in the  $(Se_2)$  arm of  $(GeSe_5)^{4-}$ . Definitive assignments can only be made by normal-mode analysis. However, in  $K_2EuSiSe_5$ , the most intense peak was found at  $234\text{ cm}^{-1}$ , indicating a reasonable assignment for the  $(SiSe_5)^{4-}$  pseudotetrahedral symmetric stretch. This peak is broad enough to obscure the higher energy Se–Se stretch around  $250\text{ cm}^{-1}$ . Figure 6 shows the Raman spectrum for  $KEuGeS_4$ . The large peak at  $380.0\text{ cm}^{-1}$  is assigned to the totally symmetric stretch of the tetrahedral  $(GeS_4)^{4-}$  unit. Low energy phonons in these spectra could be related to a variety of different lattice motions including rigid body motion of the tetrahedra, but the well-behaved thermal ellipsoids in the single-crystal X-ray analysis did not indicate

(48) Briggs Piccoli, P. M.; Abney, K. D.; Schoonover, J. R.; Dorhout, P. K. *Inorg. Chem.* **2000**, *39*, 2970–2976.

any motion of this type. Table 6 lists the Raman peaks for  $\text{K}_2\text{EuGeSe}_5$  and  $\text{KEuGeS}_4$ .

UV–Vis optical band-gap analysis of compounds **I**–**IV** shows that  $\text{K}_2\text{EuSiSe}_5$ ,  $\text{K}_2\text{EuGeSe}_5$ ,  $\text{KEuSiS}_4$ , and  $\text{KEuGeS}_4$  are all likely semiconductors with optical band-gaps of 2.00, 1.84, 1.72, and 1.71 eV, respectively. Figures 7 and 8 show the optical band-gap curves for  $\text{K}_2\text{EuGeSe}_5$  and  $\text{KEuGeS}_4$ , respectively.

Fluorescence spectroscopy was performed on compounds **III** and **IV**. Fluorescence emission is expected in the red region of the spectrum if Eu(III) is indeed present in these compounds.<sup>49</sup> When a 327 nm excitation wavelength was used, intense Eu(III) fluorescence was observed at 614 nm in both compounds. The emission spectra for  $\text{KEuSiS}_4$  and  $\text{KEuGeS}_4$  are shown in Figures 9 and 10, respectively. In  $\text{KEuGeS}_4$  the 614 nm peak is found as a shoulder on the very intense frequency doubled 654 nm peak. These peaks were not observed in either compound **I** or **II**.

## Conclusions

The quaternary compounds  $\text{K}_2\text{EuTSe}_5$  and  $\text{KEuTS}_4$  (T = Si, Ge) were synthesized under equivalent reactant ratios. The difference in structures clearly shows the effect of different

oxidizing agents on the crystalline product observed. In the selenides, we observe Se–Se bonding within the  $(\text{TSe}_5)^{4-}$  (T = Si, Ge) anionic unit. In the sulfides we observe Eu(III) which was verified using solid-state fluorescence spectroscopy. Future work includes synthesizing additional quaternary rare-earth chalcosilicates, germanates, and stannates.

**Acknowledgment.** Funding for this work was provided by the National Science Foundation (CHE-9625378 and DMR-0076180) and a NSF-MRI Instrumentation Grant.

**Supporting Information Available:** Tables of additional crystallographic details, all bond distances and angles, anisotropic thermal parameters, ORTEP plots of **I** and **III**, and the Raman spectrum of **I**. This material is free of charge via the Internet at <http://pubs.acs.org>.

IC001248S

(49) Blasse, G.; Grabmaier, B. C. *Luminescent Materials*; Springer-Verlag: New York, 1994.